EDGE ARTICLE

Check for updates

Synthesis of a terminal Ce(IV) oxo complex by photolysis of a Ce(III) nitrate complex†

Mikiyas K. Assefa, [ID] Guang Wu and Trevor W. Hayton [ID] *

Reaction of $[Ce(NR_2)_3]$ (R = SiMe$_3$) with LiNO$_3$ in THF, in the presence of 2,2,2-cryptand, results in the formation of the Ce(III) "ate" complex, $[Li(2,2,2\text{-cryptand})][Ce(\kappa^2\text{-}O_2NO)(NR_2)_3]$ (**1**) in 38% yield. Photolysis of **1** at 380 nm affords $[Li(2,2,2\text{-cryptand})][Ce(O)(NR_2)_3]$ (**2**), in 33% isolated yield after reaction work-up. Complex **2** is the first reported example of a Ce(IV) oxo complex where the oxo ligand is not supported by hydrogen bonding or alkali metal coordination. Also formed during photolysis are $[Li(2,2,2\text{-cryptand})]_2[(\mu_3\text{-}O)\{Ce(\mu\text{-}O)(NR_2)_2\}_3]$ (**3**) and $[Li(2,2,2\text{-cryptand})][Ce(OSiMe_3)(NR_2)_3]$ (**4**). Their identities were confirmed by X-ray crystallography. Complex **4** can also be prepared *via* reaction of $[Ce(NR_2)_3]$ with LiOSiMe$_3$ in THF, in the presence of 2,2,2-cryptand. When synthesized in this fashion, **4** can be isolated in 47% yield. To rationalize the presence of **2**, **3**, and **4** in the reaction mixture, we propose that photolysis of **1** first generates **2** and NO$_2$, *via* homolytic cleavage of the N–O bond in its nitrate co-ligand. Complex **2** then undergoes decomposition *via* two separate routes: (1) ligand scrambling and oligomerization to form **3**; and, (2) abstraction of a trimethylsilyl cation to form a transient Ce(IV) silyloxide, $[Ce^{IV}(OSiMe_3)(NR_2)_3]$, followed by 1e$^-$ reduction to form **4**. Alternatively, complex **4** could form directly *via* ·SiMe$_3$ abstraction by **2**.

Introduction

The past five years has seen significant progress made toward the synthesis of lanthanide complexes containing metal–ligand multiple bonds,[1–6] including those featuring Ln=N and Ln=C interactions. For example, Anwander and co-workers recently described the synthesis of the first terminal lanthanide imido complex, $[(Tp^{tBu,Me})Lu=N(3,5\text{-}(CF_3)_2C_6H_3)(DMAP)]$, *via* Lewis base-induced methane elimination.[2] Similarly, Schelter and co-workers reported the synthesis of a series of Ce(IV) imido complexes, $[ML_n][Ce=N(3,5\text{-}(CF_3)_2C_6H_3)(TriNOx)]$ (TriNOx = $N(o\text{-}CH_2C_6H_4N(^tBu)O)_3$; ML_n = Li(THF)(Et$_2$O), Li(TMEDA), K(DME)$_2$, Rb(DME)$_2$, Cs(DME)$_2$).[5] Significant progress has also been made toward the synthesis of cerium(IV) oxo complexes.[7] For example, Leung and co-workers recently reported the synthesis of a Ce(IV) oxo complex ligated by the tripodal Kläui ligand, $[(L_{OEt})_2Ce(O)(H_2O)]\cdot MeC(O)NH_2$ (**I**, L_{OEt} = CpCo$\{P(O)(OEt)_2\}_3$, Scheme 1).[3] Additionally, our group reported the synthesis of the cerium(IV) oxo complex, $[Li(12\text{-crown-}4)][(NN'_3)Ce(O)]$ (**II**, NN'$_3$ = N(CH$_2$CH$_2$NR)$_3$, R = Si^{t}BuMe$_2$), which was synthesized by thermal decomposition of a Ce(III) nitrate precursor $[Li(12\text{-crown-}4)][(NN'_3)Ce(\kappa^2\text{-}O_2NO)]$.[8] More recently,

Scheltar and co-workers reported the synthesis of a Ce(IV) oxo supported by the tripodal TriNOx ligand, $[(TriNOx)\{Ce(O)\}Rb]_4$ (**III**).[5] Also of note is $[M]_2[Ce(\mu\text{-}O)(NR_2)_3]_2$ (**IV**, M = Na, K; R = SiMe$_3$), reported by Lappert and co-workers in 2010.[9] These two complexes, which pre-date the other examples mentioned here, were isolated in low yield (*ca.* 20%) upon reaction of

Department of Chemistry and Biochemistry, University of California Santa Barbara, Santa Barbara, CA 93106, USA. E-mail: hayton@chem.ucsb.edu
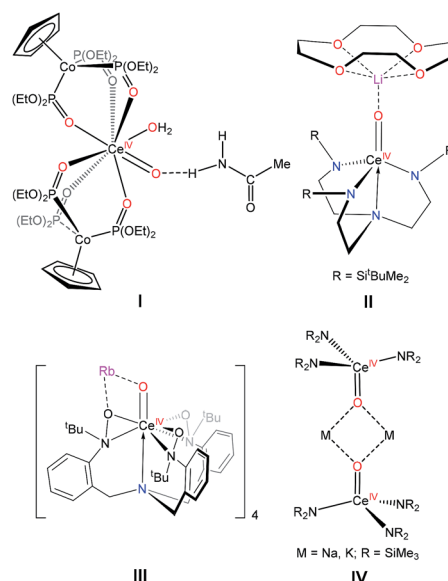
Scheme 1 Selected complexes bearing lanthanide−oxygen multiple bonds.

Ce(NR$_2$)$_3$ with MNR$_2$, in the presence of O$_2$,[9] but they were not completely characterized.

Interestingly, every cerium oxo complex isolated thus far has utilized an external non-covalent interaction to instil stability to this highly reactive functional group. For example, the Ce=O bond in **I** is stabilized by hydrogen bonding to an acetamide solvent molecule.[3] Similarly, the oxo ligands in **II** and **III** are stabilized by their interactions with a capping alkali metal counterion.[5,8] The prevalence of these non-covalent interactions can be rationalized by the poor overlap of the metal f and d orbitals with oxygen 2p orbitals, which results in weak π bonds within the Ce=O fragment, concomitant with considerable oxo nucleophilicity.[4,9–11] Indeed, controlling this nucleophilic character has been one of the key challenges to synthesizing a terminal lanthanide oxo complex.[3]

The unique redox chemistry of the lanthanides also poses a barrier for the synthesis of lanthanide oxo complexes. In particular, cerium redox chemistry is dominated by the Ce(III/IV) redox couple, and thus formation of a Ce(IV) oxo complex from a Ce(III) precursor essentially mandates a 1e$^-$ O-atom transfer process. However, traditional O-atom transfer reagents, such as N$_2$O, pyridine-N-oxide, and peroxyacids, are 2e$^-$ oxidants.[12] In our recent synthesis of [Li(12-crown-4)][(NN′$_3$)Ce(O)], the oxo ligand was formed *via* reduction of a nitrate ligand, in a formal 1e$^-$ O-atom transfer process. Several other examples demonstrating the use of nitrate as a 1e$^-$ O-atom source have emerged in recent years,[13–16] suggesting that [NO$_3$]$^-$ could be a valuable reagent for the generation of f-element oxo complexes. This mode of reactivity can also be promoted with light. For example, Berry and co-workers demonstrated that photolysis of Ru$_2$(chp)$_4$(NO$_3$) (chp = 6-chloro-2-hydroxypyridinate) generated a metal oxo with concomitant release of NO$_2$.[13] Similarly, Suslick and co-workers reported that photolysis of Mn(TPP)(NO$_3$) also resulted in metal oxo generation and release of NO$_2$.[15] However, it should be noted that in both of these examples the resulting metal oxo was unstable and not isolated.

Drawing on these results, we sought to further develop the use of [NO$_3$]$^-$ as an O-atom source for the synthesis of f-element oxo complexes. Herein, we describe the photochemical cleavage of nitrate in a Ce(III) "ate" precursor to generate the first terminal Ce(IV) oxo complex.

Results and discussion

Reaction of [Ce(NR$_2$)$_3$] (R = SiMe$_3$) with LiNO$_3$ in THF, in the presence of 2,2,2-cryptand, results in the formation of the Ce(III) "ate" complex, [Li(2,2,2-cryptand)][Ce(κ^2-O$_2$NO)(NR$_2$)$_3$] (**1**), which can be isolated as a yellow crystalline solid in 38% yield after work-up (eqn (1)). The ^{1}H NMR spectrum of **1** in py-d_5 displays a broad singlet at −1.32 ppm, assignable to the SiMe$_3$ environment, and three resonances at 2.48, 3.45 and 3.51 ppm, assignable to the cryptand moiety. The chemical shift of the methyl resonance, along with its broad appearance, support the presence of a paramagnetic Ce(III) centre in this complex. The ^{7}Li{^{1}H} NMR spectrum reveals a broad resonance at −1.08 ppm, indicative of a single lithium environment.

$$\text{(1)}$$
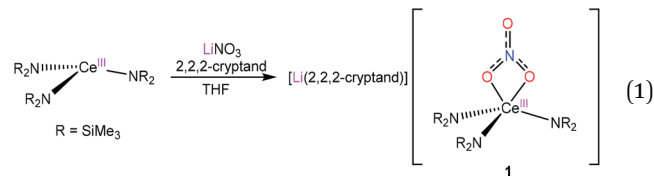
The solid-state molecular structure of **1** (Fig. 1) reveals a κ^2 coordination mode of the nitrate ligand, similar to that observed for the cerium(III) nitrate TREN complex, [Li(12-crown-4)][(NN′$_3$)Ce(NO$_3$)].[8] However, the Ce–O distances in **1** (2.653(2) and 2.562(2) Å) are shorter than those observed for [Li(12-crown-4)][(NN′$_3$)Ce(NO$_3$)] (2.724(6) and 2.745(6) Å), likely because of the bulkier TREN ligand in the latter and the absence of Li–O interactions in the former. In addition, the Ce–N distances in **1** (2.367(2)–2.398(2) Å) are consistent with the Ce–N distances reported for other Ce(III) amido complexes.[17–20] For comparison, the Ce–N distances in Ce(TMP)$_3$(THF) (TMP = 2,2,6,6-tetramethylpiperidinato) range from 2.346(2)–2.374(2) Å, while the distances in [Li(THF)][Ce(NCy$_2$)$_4$] range from 2.320(2)–2.330(2) Å.[18,19] The lithium counter-ion in **1** is encapsulated by the 2,2,2-cryptand moiety, rendering **1** a separated cation–anion pair. Interestingly, only five of the eight donor atoms in the cryptand moiety are bound to the lithium ion; two nitrogen atoms and one oxygen atom remain uncoordinated. Similar binding modes have been observed in other [Li(2,2,2-cryptand)]$^+$ complexes.[21–24]

With complex **1** in hand, we explored its suitability as a Ce(IV) oxo precursor. Unlike [Li(12-crown-4)][(NN′$_3$)Ce(NO$_3$)], however, which is mostly consumed upon standing at room temperature for 24 h, we discovered that complex **1** is not especially temperature sensitive. A py-d_5 solution of **1**, which was stored
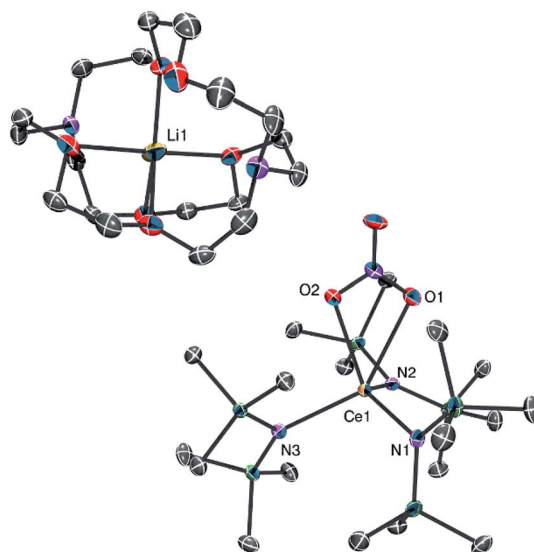
Fig. 1 ORTEP diagram of **1** shown with 50% probability ellipsoids. Hydrogen atoms are omitted for clarity. Selected bond distances (Å) and angles (°): Ce1–O1 = 2.653(2), Ce1–O2 = 2.562(2), Ce1–N1 = 2.385(3), Ce1–N2 = 2.367(2), Ce1–N3 = 2.398(2), N2–Ce1–N1 = 121.01(8), N2–Ce1–N3 = 112.82(8), N1–Ce1–N3 = 101.96(9).

for 24 h at room temperature in the absence of light, still consisted primarily of complex **1**, as determined by ^{1}H NMR spectroscopy. However, we do observe the formation of several new species in this sample, in small amounts, as revealed by resonances at 0.69, 0.20, and −0.58 ppm (see Fig. S10 in the ESI†). These were later identified as belonging to [Li(2,2,2-cryptand)][Ce(O)(NR$_2$)$_3$] (**2**), [Li(2,2,2-cryptand)]$_2$[(μ$_3$-O){Ce(μ-O)(NR$_2$)$_2$}$_3$] (**3**), and [Li(2,2,2-cryptand)][Ce(OSiMe$_3$)(NR$_2$)$_3$] (**4**), respectively (*vide infra*). These three complexes were present in a relative ratio of 2 : 27 : 1. The relatively high thermal stability of **1** led us to conclude that formation of a terminal Ce(IV) oxo complex through thermal activation of the nitrate co-ligand in **1** was not synthetically viable.

Given the relatively high thermal stability of **1**, we sought an alternative route to reduce its nitrate co-ligand. Schelter and co-workers previously reported that photolysis of [Ce(NR$_2$)$_3$] resulted in formation of a relatively long-lived excited state.[25,26] This excited state species is strongly reducing, and can elicit homolytic cleavage of the C–Cl bond in PhCH$_2$Cl, resulting in formation of [Ce(Cl)(NR$_2$)$_3$] and bibenzyl.[25] The UV-vis spectrum of **1** features two absorptions at 380 nm ($\varepsilon = 200$ M^{-1} cm^{-1}) and 336 nm ($\varepsilon = 140$ M^{-1} cm^{-1}) (Fig. S14†), and is similar to that reported for [Ce(NR$_2$)$_3$].[25] We have assigned the former absorption to a metal-based 4f → 5d$_{z^2}$ transition and the latter to a 4f → 5d$_{xz/yz}$ transition, by analogy with the assignments reported for [Ce(NR$_2$)$_3$]. For comparison, these transitions occur at 413 nm and 341 nm, respectively, in [Ce(NR$_2$)$_3$]. We attribute the *ca.* 30 nm blue shift observed for the 4f → 5d$_{z^2}$ transition in **1** to the presence of the additional nitrate co-ligand, as well as its overall negative charge.

Given the similar optical properties of **1** and [Ce(NR$_2$)$_3$], we hypothesized that photolysis of **1** would induce reduction of the nitrate ligand to afford a Ce(IV) oxo complex. To this end, a 2 : 1 tol-d_8/py-d_5 solution of **1**, in an NMR tube equipped with a J-Young valve, was exposed to light from a 380 nm LED lightstrip for 6 h at −5 °C (Scheme 2). A ^{1}H NMR spectrum of this sample revealed an approximately 80% consumption of **1**, as evidenced by the attenuation of its SiMe$_3$ resonance at −1.18 ppm. In addition, we observe the appearance of a sharp singlet at 0.80 ppm, as well as the appearance of broad singlets at 0.28, −0.21, and −0.43 ppm (see Fig. S3 in ESI†). We assigned

Scheme 2 Synthesis of complexes **2**, **3**, and **4** *via* photolysis of **1**.

the sharp singlet at 0.80 ppm to the terminal Ce(IV) oxo complex [Li(2,2,2-cryptand)][Ce(O)(NR$_2$)$_3$] (**2**), while we have tentatively assigned the resonance at 0.28 ppm to the Ce(IV) oxo cluster [Li(2,2,2-cryptand)]$_2$[(μ$_3$-O){Ce(μ-O)(NR$_2$)$_2$}$_3$] (**3**). In addition, the resonances at −0.21 and −0.43 ppm, which integrate to 9 and 54 protons, respectively, are assignable to the Ce(III) silyloxide [Li(2,2,2-cryptand)][Ce(OSiMe$_3$)(NR$_2$)$_3$] (**4**). After 6 h of photolysis, these three species were present in an approximately 11 : 2.5 : 1 ratio, according to NMR spectroscopy (Fig. S4†). Attempts to photolyse the reaction mixture for longer times, in an attempt to get complete consumption of **1**, lead to decreased yields of **2**. We also found that the use of the 2 : 1 tol-d_8/py-d_5 solvent system was critical to maximize the amount of **2** formed in the reaction mixture. If we perform the photolysis in neat py-d_5, the relative amount of **2** decreased substantially; under these conditions complexes **2** and **3** are formed in nearly equal amounts. Moreover, photolyses performed in neat tol-d_8 proved impractical because of the low solubility of complex **1** in that solvent. Finally, we observed that photolyses conducted in NMR tubes result in the most efficient consumption of **1**, likely due to their high surface-to-volume ratio.

Work-up of the reaction mixture resulted in the isolation of complex **2** as yellow plates in 33% yield. Its formulation was confirmed by X-ray crystallography (see below). In one instance, we also observed the deposition of small amounts of pale yellow crystals and colorless plates, which were subsequently identified as **3** and **4**, respectively, by X-ray crystallography.

Complex **2** crystallizes in the monoclinic space group $P2_1/c$ (Fig. 2). In the solid state, **2** displays a terminal Ce=O linkage and a pseudo-tetrahedral geometry about the cerium centre. Its Ce–O bond length (1.840(7) Å) is shorter than those observed for **II** (1.902(2) Å), **III** (1.887(4)–1.902(4) Å), and **IV** (1.908(3) Å),[5,8,9] possibly because of the absence of any alkali metal–oxo interaction in **2**.[5,8] The Ce–O distance in **2** is also shorter than that calculated for [K(18-crown-6)][Ce(O)(NR$_2$)$_3$] (1.904 Å), which also features an alkali metal–oxo interaction.[8] Interestingly, however, the Ce–O distance in **2** is identical to that observed for hydrogen-bond stabilized **I** (1.857(3) Å) by the 3σ criterion,[3] suggesting that the hydrogen bonding interaction in **I** does not substantially disrupt the Ce=O bond. Also of note, the Ce–N distances in **2** (2.353(8)–2.397(8) Å) are slightly longer than those reported for other Ce(IV) amides. For example, the Ce–N distances in Ce(NCy$_2$)$_4$ range from 2.238(5) to 2.247(6) Å, while those of [Ce(X)(NR$_2$)$_3$] (X = Cl, Br) are 2.217(3) and 2.219(7) Å, respectively.[19,27,28] This lengthening may be a consequence of the strongly donating nature of the oxo ligand, along with the complex's overall negative charge, which weakens the Ce–N bonds. For further comparison, [Li(12-crown-4)][(NN′$_3$)Ce(O)] also features longer than expected Ce–N distances.[8] Finally, the Li-binding mode of the 2,2,2-cryptand moiety in **2** is similar to that observed in **1**. However, in **2**, six of the eight donor atoms in the cryptand moiety are bound to the lithium ion; only one nitrogen atom and one oxygen atom remain uncoordinated.

Complex **2** is soluble in toluene, Et$_2$O, benzene, and pyridine, but decomposes when exposed to THF, acetonitrile, and dichloromethane (forming HN(SiMe$_3$)$_2$ as the only identifiable product). Its ^{1}H NMR spectrum in py-d_5 features a sharp singlet
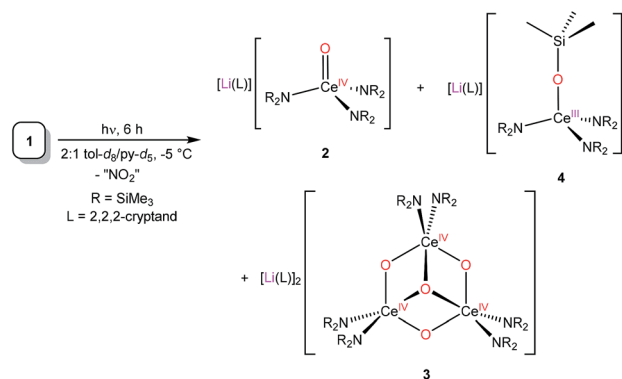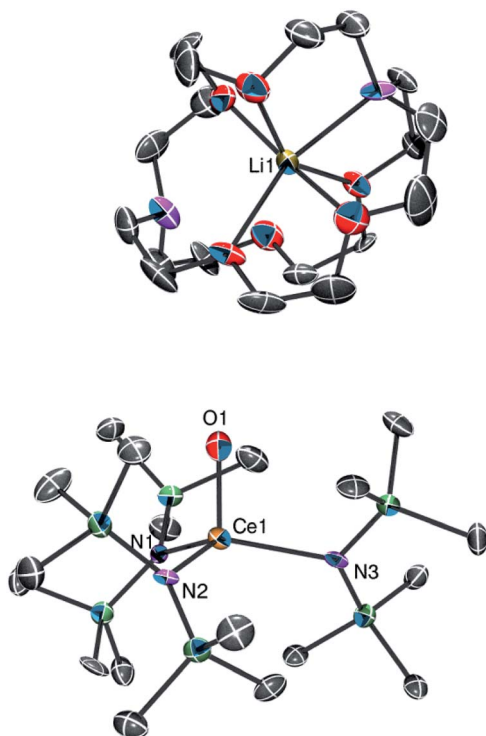
Fig. 2 ORTEP diagram of **2** shown with 50% probability ellipsoids. Hydrogen atoms are omitted for clarity. Selected bond distances (Å) and angles (°): Ce1–O1 = 1.840(7), Ce1–N1 = 2.397(8), Ce1–N2 = 2.353(8), Ce1–N3 = 2.383(8), N2–Ce1–N1 = 116.4(3), N3–Ce1–N1 = 113.4(3), N2–Ce1–N3 = 116.8(3), O1–Ce1–N1 = 103.9(3), O1–Ce1–N2 = 101.7(3), O1–Ce1–N3 = 101.5(3).

Fig. 3 ORTEP diagram of **3** shown with 50% probability ellipsoids. Hydrogen atoms, diethyl ether solvate and two [Li(2,2,2-cryptand)] counter-ions are omitted for clarity. Selected bond distances (Å) and angles (°): Ce1–O1 = 2.294(7), Ce1–O2 = 2.078(7), Ce1–O4 = 2.133(7), Ce2–O1 = 2.310(7), Ce2–O3 = 2.109(7), Ce2–O4 = 2.071(7), Ce3–O1 = 2.289(7), Ce3–O2 = 2.130(7), Ce3–O3 = 2.100(7), Ce1–N1 = 2.391(8), Ce1–N2 = 2.366(8), Ce2–N5 = 2.389(8), Ce2–N6 = 2.380(9), Ce3–N3 = 2.386(9), Ce3–N4 = 2.415(9), Ce3–O1–Ce1 = 99.8(3), Ce3–O1–Ce2 = 99.6(3), Ce1–O1–Ce2 = 99.5(3).

at 0.69 ppm integrating to 54 protons, which is assignable to the $SiMe_3$ environment, while the resonances at 2.56, 3.52, and 3.59 ppm, each integrating to 12 protons, are assignable to the cryptand moiety. The chemical shift of its $SiMe_3$ resonance is nearly identical to that assigned to this complex in the spectrum of the crude reaction mixture (Fig. S4†). The $^7Li\{^1H\}$ NMR spectrum of **2** features a broad singlet centred at −1.00 ppm. This chemical shift is in the range previously reported for the [Li(2,2,2-cryptand)]$^+$ ion.[29,30] We also recorded the Raman spectrum of **2**, but were unable to make a definitive assignment of the Ce=O stretch. Finally, we have found that complex **2** is somewhat thermally sensitive. Upon standing in 2 : 1 tol-d_8/py-d_5 at room temperature for 4 d, complex **2** decomposes to a mixture of **3**, **4**, and $LiN(SiMe_3)_2$ (along with other unidentified products) with about 70% conversion (Fig. S12 and S13†). Under these conditions, complexes **3** and **4** are present in an approximately 3 : 1 ratio. Similar results are observed when **2** is left to stand in neat py-d_5 (Fig. S11†).

Complex **3** crystallizes in triclinic space group $P\bar{1}$ (Fig. 3). In the solid state, complex **3** consists of a partial cubane Ce_3O_4 core. Each Ce centre is also ligated by two silylamide ligands. Additionally, **3** features two [Li(2,2,2-cryptand)]$^+$ counterions, confirming the tetravalent oxidation state of each cerium atom. The Ce–O distances observed for the three μ_2-oxo ligands in **3** range from 2.071(7) to 2.133(7) Å, and are comparable to those observed in the structurally related Ce(IV) oxo cluster, [{(μ-O)
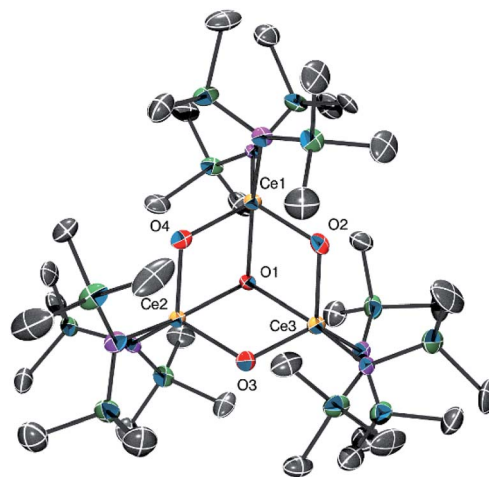
$Ce(NR_2)_2\}_3$],[9] reported by Lappert and co-workers. The Ce–O distances observed for the μ_3-oxo ligand in **3** are longer, ranging from 2.289(7) to 2.310(7)Å, but are similar to those reported for other known [$Ce_3(\mu_3$-oxo)] clusters.[31,32] We can rule out the presence of a hydroxo ligand in **3** on the basis of our structural data. In particular, the Ce–O distances of μ_2- or μ_3-hydroxo ligands are anticipated to be substantially longer than the Ce–O distances observed for **2**.[33,34] As was observed for **2**, the Ce–N distances in **3** (2.366(8)–2.415(9) Å) are somewhat longer than those typically reported for Ce(IV) amides.[19,27,28] Unfortunately, we have been unable to isolate pure samples of **3**, and thus have been unable to complete its characterization. As such, the NMR spectroscopic assignments that we report for this complex (see above) should be considered tentative.

Complex **4** crystallizes in the monoclinic space group $P2_1/n$ and its solid-state molecular structure is shown in Fig. 4. In the solid state, complex **4** consists of a pseudo-tetrahedral Ce(III) anion and a [Li(2,2,2-cryptand)]$^+$ cation. Complex **4** features a Ce–O bond length of 2.214(3) Å which is significantly longer than the Ce–O distance found in **2** (1.840(7) Å), further supporting the presence of Ce=O multiple bond character in the latter. However, this distance is similar to the average Ce–O$_{SiPh_3}$ distance in $Ce(OSiPh_3)_3(THF)_3$ (2.22 Å).[35] The average Ce–N distance in **4** (2.41 Å) is comparable to that observed for **1** (2.38 Å), consistent with its anticipated Ce(III) oxidation state. Finally, the Ce–O–Si bond angle (178.9(2)°) is similar to that observed for $Ce(OSiPh_3)_3(THF)_3$ (av. 174°)[35] and [$(NN'_3)Ce(OSiMe_2{}^tBu)$] (167.2(2)°).[8]

Conveniently, complex **4** can be synthesized independently *via* reaction of [$Ce(NR_2)_3$] with $LiOSiMe_3$ in THF, in the presence of 2,2,2-cryptand (eqn (2)), permitting its complete
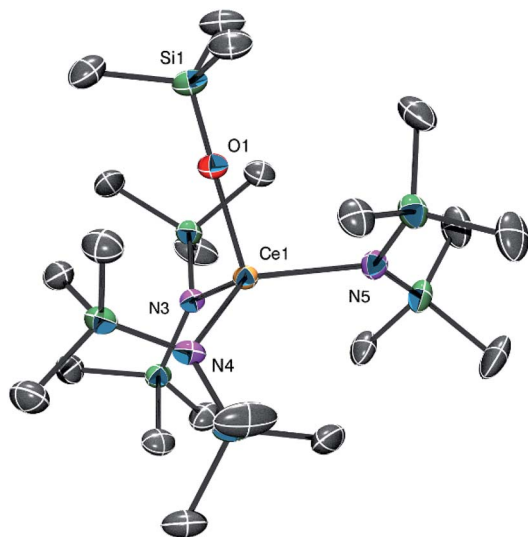
Fig. 4 ORTEP diagram of **4** shown with 50% probability ellipsoids. Hydrogen atoms and [Li(2,2,2-cryptand)] counterion are omitted for clarity. Selected bond distances (Å) and angles (°): Ce1–O1 = 2.214(3), Ce1–N3 = 2.430(4), Ce1–N4 = 2.396(4), Ce1–N5 = 2.413(4), O1–Si1 = 1.607(4), N4–Ce1–N3 = 109.97(13), N4–Ce1–N5 = 117.68(14), N5–Ce1–N3 = 117.42(13), Si1–O1–Ce1 = 178.9(2).

characterization. Synthesized *via* this route, **4** can be isolated as a white solid in 47% yield after work-up.
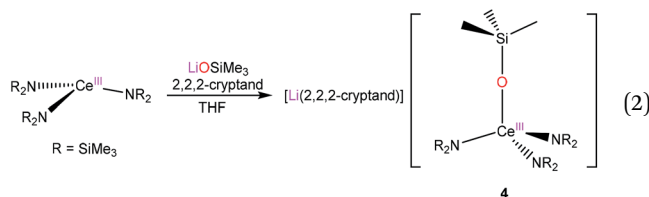
The ^{1}H NMR spectrum of **4** in py-d_5 features two broad singlets at −0.37 and −0.59 ppm, integrating to 9 and 54 protons, respectively. These resonances are assignable to the OSiMe$_3$ and N(SiMe$_3$)$_2$ methyl environments, respectively. Importantly, these resonances are nearly identical to those assigned to this complex in the spectrum of crude reaction mixture (Fig. S4†). Also observed in the ^{1}H NMR spectrum of **4** are resonances at 2.56, 3.52 and 3.60 ppm, each integrating to 12 protons, which are assignable to the cryptand moiety. Finally, its ^{7}Li{^{1}H} NMR spectrum consists of a single resonance at −0.97 ppm.

To rationalize the presence of **2**, **3**, and **4** in the reaction mixture, we propose that photolysis of **1** first generates **2** and NO$_2$, *via* homolytic cleavage of the N–O bond in its nitrate co-ligand. However, **2** is unstable to the reaction conditions and begins to decompose *via* two separate routes: (1) ligand scrambling and oligomerization to form **3**; and, (2) abstraction of a trimethylsilyl cation to form a transient Ce(iv) silyloxide, [Ce^{IV}(OSiMe$_3$)(NR$_2$)$_3$], followed by 1e$^-$ reduction to form **4**. Alternatively, complex **4** could form directly *via* ·SiMe$_3$ abstraction by **2**. To support these hypotheses, we note that complex **2** is thermally unstable, and slowly decomposes to

form a mixture of **3** and **4** in solution (Fig. S12 and S13†). Additionally, we observe a minor resonance at 0.53 ppm in the ^{1}H NMR spectrum of the photolysis reaction mixture (Fig. S4†), which is assignable to LiN(SiMe$_3$)$_2$. Its presence is consistent with the proposed conversion of **2** to **3** *via* ligand scrambling and loss of LiN(SiMe$_3$)$_2$. Finally, we previously demonstrated that the Ce(iv) silyloxide, [(NN$'_3$)Ce(OSi^{t}BuMe$_2$)], was formed as a minor by-product during the conversion of [Li(12-crown-4)] [(NN$'_3$)Ce(κ^2-O$_2$NO)] to the Ce(iv) oxo, [Li(12-crown-4)][(NN$'_3$) Ce(O)],[8] presumably *via* a similar adventitious [SiR$_3$]$^+$ abstraction.

To test the thermodynamic favourability of the proposed 1e$^-$ reduction to form **4**, we investigated its electrochemistry by cyclic voltammetry. The cyclic voltammogram of **4** in THF reveals a redox feature centred at −0.53 V at 200 mV s^{-1} (*vs.* Fc/Fc$^+$; see Fig. S23 in ESI†). This feature is marked by a large difference between the potentials of the oxidation and reduction peaks (*i.e.*, 0.72 V at 200 mV s^{-1}), suggestive of an ECE-type process. While the potential of this feature is comparable to those previously reported for cerium complexes with similar ligand frameworks, including [Ce(F)(NR$_2$)$_3$] (−0.56 V), [Ce(Cl)(NR$_2$)$_3$] (−0.30 V) and [Ce(Br)(NR$_2$)$_3$] (−0.31 V),[36–38] its electrochemical irreversibility suggests that [Ce^{IV}(OSiMe$_3$)(NR$_2$)$_3$] is not particularly stable. Therefore, complex **4** may not be formed *via* a straightforward 1e$^-$ reduction of a [Ce^{IV}(OSiMe$_3$)(NR$_2$)$_3$] intermediate. Instead, the cyclic voltammetry data may be evidence for a concerted ·SiMe$_3$ abstraction by **2** to form **4**. A similar ·SiMe$_3$ abstraction by the uranyl fragment has been reported by Arnold and co-workers.[39–41]

Conclusions

In summary, we report the synthesis of the first lanthanide oxo complex where the oxo ligand is not supported by hydrogen bonding or alkali metal coordination, namely, [Li(2,2,2-crypt-and)][Ce(O)(NR$_2$)$_3$] (**2**). This complex was generated by photolysis of the Ce(iii) nitrate precursor [Li(2,2,2-cryptand)][Ce(κ^2-O$_2$NO)(NR$_2$)$_3$] (**1**), which results in photochemical cleavage of the nitrate co-ligand. Also formed in the photolysis reaction are the Ce(iv) oxo cluster, [Li(2,2,2-cryptand)]$_2$[(μ_3-O){Ce(μ-O)(NR$_2$)$_2$}$_3$] (**3**), and the Ce(iii) silyloxide complex, [Li(2,2,2-cryptand)][Ce(OSiMe$_3$)(NR$_2$)$_3$] (**4**). We believe these two complexes are formed upon thermal (or photochemical) decomposition of **2** after its initial generation in the reaction mixture. Overall, this work further highlights the utility of [NO$_3$]$^-$ as a 1e$^-$ O-atom source for the generation of lanthanide oxo complexes. Indeed, we have now shown that nitrate reduction to form cerium oxos can proceed *via* both thermal and photochemical routes. Going forward, we will attempt to synthesize a Ln(iii) oxo complex *via* 1e$^-$ O-atom transfer from [NO$_3$]$^-$. This is anticipated to be a greater synthetic challenge because the lower Ln oxidation state results in reduced Ln–O bond covalency.[42]

Conflicts of interest

There are no conflicts to declare.

Acknowledgements

Notes and references

1 M. Gregson, E. Lu, J. McMaster, W. Lewis, A. J. Blake and S. T. Liddle, *Angew. Chem., Int. Ed.*, 2013, **52**, 13016–13019.

2 D. Schädle, M. Meermann-Zimmermann, C. Schädle, C. Maichle-Mössmer and R. Anwander, *Eur. J. Inorg. Chem.*, 2015, **2015**, 1334–1339.

3 Y.-M. So, G.-C. Wang, Y. Li, H. H. Y. Sung, I. D. Williams, Z. Lin and W.-H. Leung, *Angew. Chem., Int. Ed.*, 2014, **53**, 1626–1629.

4 O. T. Summerscales and J. C. Gordon, *RSC Adv.*, 2013, **3**, 6682–6692.

5 L. A. Solola, A. V. Zabula, W. L. Dorfner, B. C. Manor, P. J. Carroll and E. J. Schelter, *J. Am. Chem. Soc.*, 2017, **139**, 2435–2442.

6 L. A. Solola, A. V. Zabula, W. L. Dorfner, B. C. Manor, P. J. Carroll and E. J. Schelter, *J. Am. Chem. Soc.*, 2016, **138**, 6928–6931.

7 Y.-M. So, Y. Li, K.-C. Au-Yeung, G.-C. Wang, K.-L. Wong, H. H. Y. Sung, P. L. Arnold, I. D. Williams, Z. Lin and W.-H. Leung, *Inorg. Chem.*, 2016, **55**, 10003–10012.

8 P. L. Damon, G. Wu, N. Kaltsoyannis and T. W. Hayton, *J. Am. Chem. Soc.*, 2016, **138**, 12743–12746.

9 M. P. Coles, P. B. Hitchcock, A. V. Khvostov, M. F. Lappert, Z. Li and A. V. Protchenko, *Dalton Trans.*, 2010, **39**, 6780–6788.

10 J. Hong, L. Zhang, X. Yu, M. Li, Z. Zhang, P. Zheng, M. Nishiura, Z. Hou and X. Zhou, *Chem.–Eur. J.*, 2011, **17**, 2130–2137.

11 J. Scott, H. Fan, B. F. Wicker, A. R. Fout, M.-H. Baik and D. J. Mindiola, *J. Am. Chem. Soc.*, 2008, **130**, 14438–14439.

12 R. H. Holm, *Chem. Rev.*, 1987, **87**, 1401–1449.

13 A. R. Corcos, J. S. Pap, T. Yang and J. F. Berry, *J. Am. Chem. Soc.*, 2016, **138**, 10032–10040.

14 R. J. Radford, M. D. Lim, R. S. D. Silva and P. C. Ford, *J. Coord. Chem.*, 2010, **63**, 2743–2749.

15 K. S. Suslick and R. A. Watson, *Inorg. Chem.*, 1991, **30**, 912–919.

16 R. D. Taylor, P. G. Todd, N. D. Chasteen and J. T. Spence, *Inorg. Chem.*, 1979, **18**, 44–48.

17 S. D. Daniel, J.-S. M. Lehn, J. D. Korp and D. M. Hoffman, *Polyhedron*, 2006, **25**, 205–210.

18 P. B. Hitchcock, Q.-G. Huang, M. F. Lappert and X.-H. Wei, *J. Mater. Chem.*, 2004, **14**, 3266–3273.

19 P. B. Hitchcock, M. F. Lappert and A. V. Protchenko, *Chem. Commun.*, 2006, 3546–3548.

20 D. Schneider, T. Spallek, C. Maichle-Mossmer, K. W. Tornroos and R. Anwander, *Chem. Commun.*, 2014, **50**, 14763–14766.

21 A. N. Chekhlov, *Russ. J. Coord. Chem.*, 2003, **29**, 828–832.

22 R. E. A. Dillon, C. L. Stern and D. F. Shriver, *Solid State Ionics*, 2000, **133**, 247–255.

23 A. Moores, L. Ricard, P. Le Floch and N. Mézailles, *Organometallics*, 2003, **22**, 1960–1966.

24 P. A. Rudd, N. Planas, E. Bill, L. Gagliardi and C. C. Lu, *Eur. J. Inorg. Chem.*, 2013, **2013**, 3898–3906.

25 H. Yin, P. J. Carroll, J. M. Anna and E. J. Schelter, *J. Am. Chem. Soc.*, 2015, **137**, 9234–9237.

26 H. Yin, P. J. Carroll, B. C. Manor, J. M. Anna and E. J. Schelter, *J. Am. Chem. Soc.*, 2016, **138**, 5984–5993.

27 O. Eisenstein, P. B. Hitchcock, A. G. Hulkes, M. F. Lappert and L. Maron, *Chem. Commun.*, 2001, 1560–1561.

28 P. B. Hitchcock, A. G. Hulkes and M. F. Lappert, *Inorg. Chem.*, 2004, **43**, 1031–1038.

29 E. Pasgreta, R. Puchta, M. Galle, N. van Eikema Hommes, A. Zahl and R. van Eldik, *J. Inclusion Phenom. Macrocyclic Chem.*, 2007, **58**, 81–88.

30 R. R. Rhinebarger and A. I. Popov, *Polyhedron*, 1988, **7**, 1341–1347.

31 H. C. Aspinall, J. Bacsa, A. C. Jones, J. S. Wrench, K. Black, P. R. Chalker, P. J. King, P. Marshall, M. Werner, H. O. Davies and R. Odedra, *Inorg. Chem.*, 2011, **50**, 11644–11652.

32 J. Schläfer, S. Stucky, W. Tyrra and S. Mathur, *Inorg. Chem.*, 2013, **52**, 4002–4010.

33 J.-S. M. Lehn and D. M. Hoffman, CCDC 272487: CSD Communication, 2014, DOI: 10.5517/cc94jxv.

34 L. Natrajan, J. Pécaut, M. Mazzanti and C. LeBrun, *Inorg. Chem.*, 2005, **44**, 4756–4765.

35 P. S. Gradeff, K. Yunlu, T. J. Deming, J. M. Olofson, R. J. Doedens and W. J. Evans, *Inorg. Chem.*, 1990, **29**, 420–424.

36 J. R. Robinson, P. J. Carroll, P. J. Walsh and E. J. Schelter, *Angew. Chem., Int. Ed.*, 2012, **51**, 10159–10163.

37 U. J. Williams, P. J. Carroll and E. J. Schelter, *Inorg. Chem.*, 2014, **53**, 6338–6345.

38 U. J. Williams, J. R. Robinson, A. J. Lewis, P. J. Carroll, P. J. Walsh and E. J. Schelter, *Inorg. Chem.*, 2014, **53**, 27–29.

39 P. L. Arnold, D. Patel, C. Wilson and J. B. Love, *Nature*, 2008, **451**, 315–317.

40 A. Yahia, P. L. Arnold, J. B. Love and L. Maron, *Chem. Commun.*, 2009, 2402–2404.

41 A. Yahia, P. L. Arnold, J. B. Love and L. Maron, *Chem.–Eur. J.*, 2010, **16**, 4881–4888.

42 M. W. Löble, J. M. Keith, A. B. Altman, S. C. E. Stieber, E. R. Batista, K. S. Boland, S. D. Conradson, D. L. Clark, J. Lezama Pacheco, S. A. Kozimor, R. L. Martin, S. G. Minasian, A. C. Olson, B. L. Scott, D. K. Shuh, T. Tyliszczak, M. P. Wilkerson and R. A. Zehnder, *J. Am. Chem. Soc.*, 2015, **137**, 2506–2523.